Development of 3D-printed abdominal phantom for quality assurance applications

Everjoy Mones[1,2,3,4*], Ermias Beyene[1,2,3,4], Jacek Cichy[5], Adriana Zlahoda-Huzior[5], Tevfik Kaplanoglu[2,3,4], Paweł Moskal[2,4], Ewa Stępień[1,4]

[1]Department of Medical Physics, Faculty of Physics, Astronomy, and Applied Computer Science, Jagiellonian University, Kraków, Poland
[2]Department of Experimental Particle Physics and Applications, Faculty of Physics, Astronomy, and Applied Computer Science, Jagiellonian University, Kraków, Poland
[3]Doctoral School of Exact and Natural Sciences, Jagiellonian University, Kraków, Poland
[4]Center for Theranostics, Jagiellonian University, Kraków, Poland
[5]SimHub by Virmed, Al. Plk. Wł. Beliny-Prazmowskiego, Kraków, Poland
*everjoy.mones@doctoral.uj.edu.pl

Introduction

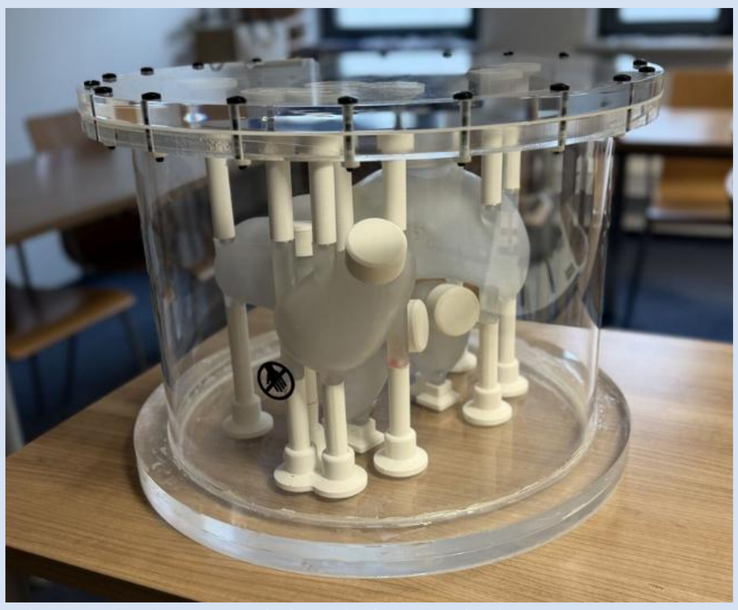


Figure 1. Image of the abdominal phantom in an upright position

3D-printed Anthropomorphic Phantom

- Provides a realistic simulation of selected human anatomical structures or region of interest
- 3D printing process enables the selection of material composition and precise control of complex anatomical structures
- Can be used to verify the radiation-emitting equipment's image quality

***Aim:* Develop a customized 3D-printed phantom of the upper abdomen region and characterize the phantom by obtaining its volumetric image without and with water using a diagnostic CT scanner**

Methodology

Phantom design and fabrication

- **Organ models' shells** (right and left kidneys, liver, spleen, stomach) – UV-resin, SLA 3D-printing
- **Organ model holders** – PLA, FDM technique
- **Cylindrical outer shell** – PMMA, CNC machining

CT image acquisition of 3D-printed phantom

- **CT scanner:** Siemens Healthineers, SOMATOM go.Top in AEC mode
- **Filling:** Without and with DI water
- **kVs:** 70, 100, 120, 140
- **Slice thickness:** 0.6mm, 1mm, 3mm

ROI analysis using RadiAnt DICOM Viewer

- **Software:** RadiAnt DICOM Viewer (Version 2025.2, 64 bit)
- **ROI Analysis:** Circular 3.0 cm^2 regions of interest (ROIs) were selected in different areas of the axial slices of the phantom images (inside and outside the organ models' shells) to determine HU

Results

Table 1. Corresponding HU measurements of the phantom without and with water for varying kVs and slice thicknesses

		0.6 mm		1.0 mm		3.0 mm	
		HU (without water)	HU (with water)	HU (without water)	HU (with water)	HU (without water)	HU (with water)
kV = 70	Inside the organ models	-998.28	NA	-996.92	-8.83	-996.49	-9.25
	Outside the organ models	-996.99	NA	-995.89	-4.36	-996.42	-2.73
kV = 100	Inside the organ models	-998.56	0.102	-991.27	0.300	-991.25	0.404
	Outside the organ models	-998.07	0.792	-998.89	0.697	-997.28	0.108
kV = 120	Inside the organ models	-996.01	0.202	-994.44	-0.244	-989.17	0.091
	Outside the organ models	-997.65	-2.245	-997.76	-2.086	-996.40	-2.976
kV = 140	Inside the organ models	-999.10	-0.022	-998.19	-0.023	-998.30	0.130
	Outside the organ models	-1000.64	-3.457	-1000.58	-1.996	-999.59	-2.027

- ***Phantom without water filling:*** within -970 HU to -1005 HU tolerance range set by ACR Method specified in AAPM TG-233
- ***Phantom with water filling:*** within -5 HU to +5 HU tolerance range set by IAEA Method specified in AAPM TG-233 except for image acquisition at 70 kV inside the organ models' shells due to reduced penetrating capability of 70 kV x-ray

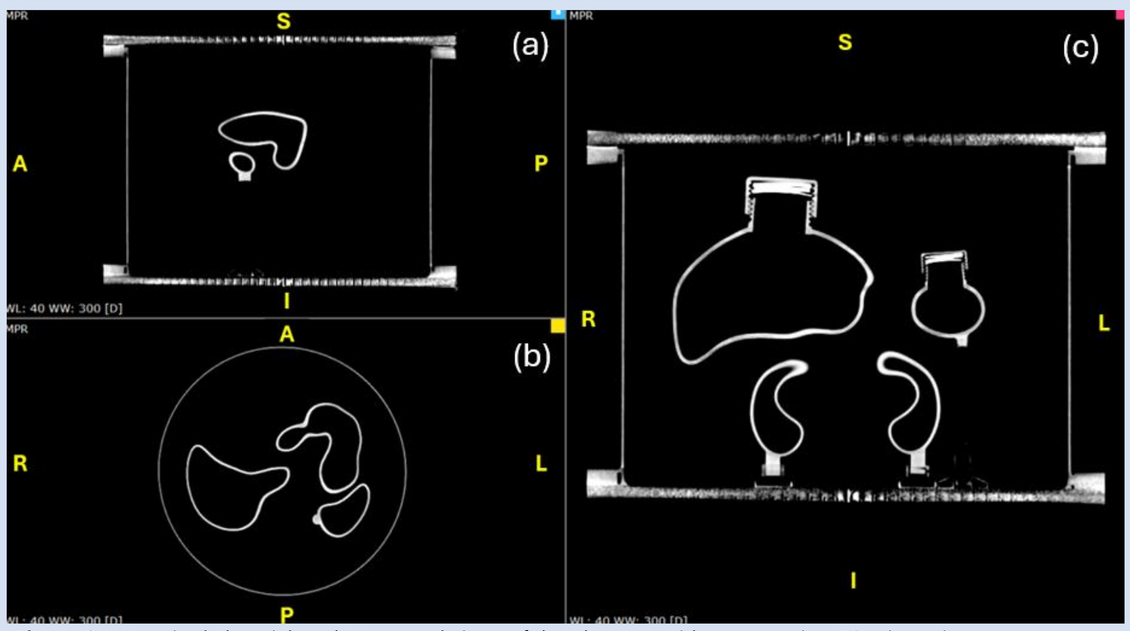


Figure 2. (a) sagittal, (b) axial, and (c) coronal views of the phantom without water in HFS orientation

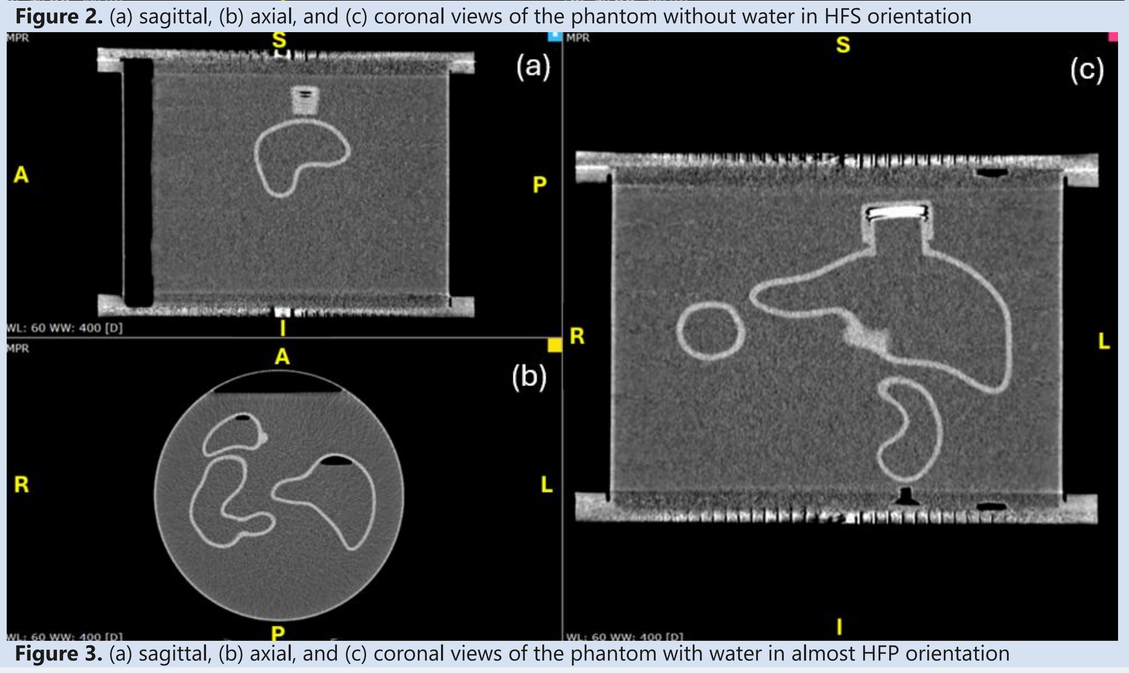


Figure 3. (a) sagittal, (b) axial, and (c) coronal views of the phantom with water in almost HFP orientation

Highlights and Recommendations

- An anthropomorphic abdominal phantom was designed and fabricated using various 3D-printing techniques and different 3D-printing materials.
- Different parameters were utilized in CT image acquisition of the phantom.
- HU measurements for every variation were within the tolerance range excluding HU values under 70 kV
- It is recommended to make use of different tissue-mimicking materials as inserts of hollow phantom organs to test phantom's capability in tests such as low contrast performance.
- Furthermore, the study aims to explore the application of the fabricated phantom in future research involving PET/CT systems for molecular and functional imaging, with particular emphasis on its potential use in the J-PET scanner.

Acknowledgements

We gratefully acknowledge support from NCN (grants 2021/42/A/ST2/00423, 2021/43/B/ST2/02150, 2022/47/I/NZ7/03112, 2023/50/E/ST2/00574), MNiSW (IAL/SP/596235/2023 and SPUB/SP/627733/2025), SciMat and qLife Priority Research Areas, ERC Advanced Grant POSITRONIUM no. 101199807, PRISMAP (Project_1729020993_aniX3), and PLGrid infrastructure (PLG/2024/017688, PLG/2025/018762).

References

1. M. Wegner, E. Gargioni, & D. Krause. (2023). Classification of phantoms for medical imaging. Procedia CIRP 119, 1140-1145
2. D. Lustermans, R. Abdulrahim, V. T. Taasti, et al. (2024). Development of a novel 3D-printed dynamic anthropomorphic thorax phantom for evaluation of four-dimensional computed tomography. Physics and Imaging in Radiation Oncology 32 100656, 1-8
3. K. Katsikari, N. Francis, N. Maalej, et al. (2024). 3D-Printed Anthropomorphic Phantom Framework for Spectral Photon-Counting CT: A Breast Phantom Application. IEEE Access 13, 6397-6412. doi: 10.1109/ACCESS.2024.3521476
4. American Association of Physicists in Medicine (AAPM). (2019). Performance evaluation of computed tomography systems: The report of AAPM Task Group 233 (AAPM Report No. 233). AAPM.
5. P. Moskal and E. Ł. Stępień. (2020). Prospects and Clinical Perspectives of Total-Body PET Using Plastic Scintillators., PET Clinics 15, 439-452